# Accepted Manuscript

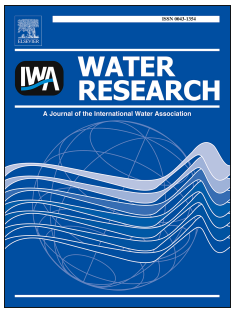


A global analysis approach for investigating structural resilience in urban drainage systems

Seith N. Mugume, Diego E. Gomez, Guangtao Fu, Raziyeh Farmani, David Butler

PII: S0043-1354(15)30014-2

DOI: 10.1016/j.watres.2015.05.030

Reference: WR 11305

To appear in: *Water Research*

Received Date: 8 December 2014

Revised Date: 1 May 2015

Accepted Date: 15 May 2015

Please cite this article as: Mugume, S.N., Gomez, D.E., Fu, G., Farmani, R., Butler, D., A global analysis approach for investigating structural resilience in urban drainage systems, Water Research (2015), doi: 10.1016/j.watres.2015.05.030.

## Global resilience analysis

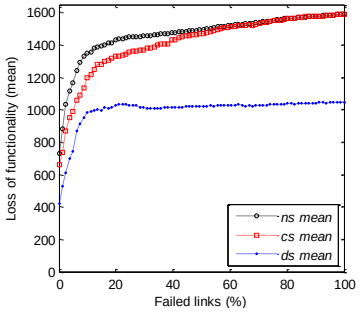


## Link failure envelopes

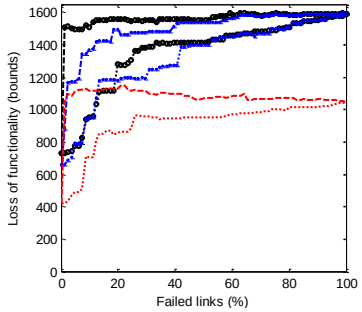


**Existing UDS**
**Centralised Storage**
**Distributed Storage**

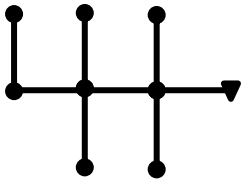

**Choose sewer modes**

- **Non-failed?**
- **Partial?**
- **Complete?**

## Resilience envelopes

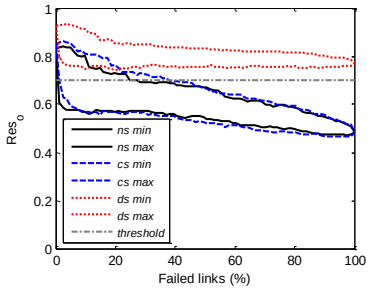

# A global analysis approach for investigating structural resilience in urban drainage systems

**Seith N. Mugume[a], Diego E. Gomez, Guangtao Fu, Raziyeh Farmani, David Butler**

[a] Centre for Water Systems, College of Engineering, Mathematics and Physical Sciences, University of Exeter, North Park Road, Exeter, EX4 4QF, United Kingdom; Tel: +44 (0)1392 723600, E-mail: snm205@exeter.ac.uk

**Abstract:** Building resilience in urban drainage systems requires consideration of a wide range of threats that contribute to urban flooding. Existing hydraulic reliability based approaches have focused on quantifying functional failure caused by extreme rainfall or increase in dry weather flows that lead to hydraulic overloading of the system. Such approaches however, do not fully explore the full system failure scenario space due to exclusion of crucial threats such as equipment malfunction, pipe collapse and blockage that can also lead to urban flooding. In this research, a new analytical approach based on global resilience analysis is investigated and applied to systematically evaluate the performance of an urban drainage system when subjected to a wide range of structural failure scenarios resulting from random cumulative link failure. Link failure envelopes, which represent the resulting loss of system functionality (impacts) are determined by computing the upper and lower limits of the simulation results for total flood volume (failure magnitude) and average flood duration (failure duration) at each link failure level. A new resilience index that combines the failure magnitude and duration into a single metric is applied to quantify system residual functionality at each considered link failure level. With this approach, resilience has been tested and characterized for an existing urban drainage system in Kampala city, Uganda. In addition, the effectiveness of potential adaptation strategies in enhancing its resilience to cumulative link failure has been tested.

**Keywords:** failure envelopes, flexibility, redundancy, resilience, structural failure, urban water management

## Nomenclature

| | |
|---|---|
| $rs_i$ | random link failure sequence |
| $ns_i$ | random failure sequences for the existing system |
| $cs_i$ | random failure sequences for the centralised storage strategy |
| $ds_i$ | random failure sequences for the distributed storage strategy |
| $N$ | total number of links |
| $n$ | Manning's roughness coefficient |
| $t_f$ | mean duration of nodal flooding |
| $t_t$ | total rainfall event duration |
| $Res_o$ | operational resilience index |
| $T$ | rainfall return period in years |
| $V_{TF}$ | total flood volume |
| $V_{TI}$ | total inflow volume |
| $\mu$ | mean |
| $\sigma$ | standard deviation |

## 1. Introduction

Recent natural and manmade catastrophic events that have led to extreme flooding in various cities worldwide have underscored the need to build resilience into existing urban drainage and flood management systems as a key strategy to minimise the resulting flooding impacts and consequences (Djordjević et al., 2011; Park et al., 2013). Urban drainage system flooding is not only caused by *external* climate-related and urbanisation threats such as extreme rainfall and increasing urbanisation but also *internal* system threats for example equipment malfunction, sewer collapse and blockages (Kellagher et al., 2009; Mugume et al., 2014; Ryu and Butler, 2008; Ten Veldhuis, 2010). System or component failures can either be abrupt (unexpected) shocks for example pump or sensor failure or chronic pressures such as asset aging and long term asset decay or sewer sedimentation. The impact of such failures, either singly or in combination on existing urban drainage infrastructure could significantly reduce the expected flood protection service levels in cities and lead to negative consequences such as loss of lives, damage to properties and critical infrastructure (Djordjević et al., 2011; IPCC, 2014; Ryu and Butler, 2008; Ten Veldhuis, 2010).

Consequently, the need to build resilience in urban drainage systems (UDSs) is increasingly recognised as vital to enhance their ability to maintain acceptable flood protection service levels in cities that they serve and to minimise the resulting flooding consequences during unexpected or exceptional loading conditions that lead to system failure (Butler et al., 2014; Djordjević et al., 2011). Although the application of concept of ***resilience*** to infrastructure systems is a recent development, there is an extensive literature on definitions and interpretation of resilience, much of which has come from the ecological systems academic community (Butler et al., 2014; Park et al., 2013). Ecological system resilience is interpreted as a measure of *system integrity* and is defined as a system's ability to maintain its basic structure and patterns of behaviour (i.e. to persist) through absorbing shocks or disturbances

under dynamic (non-equilibrium) conditions (Holling, 1996). In contrast to ecological systems, engineering systems are product of intentional human invention and are designed to provide continued (uninterrupted) services to society in an efficient manner (Blackmore and Plant, 2008; Holling, 1996; Park et al., 2013). Engineering system resilience is therefore interpreted differently from ecological resilience and focuses on ensuring *continuity and efficiency of system function* during and after failure (Butler et al., 2014; Lansey, 2012)

In the context of urban drainage, current design and rehabilitation approaches tend to focus on prevention of hydraulic (functional) failures resulting from a specified design storm of a given frequency (i.e. return period). The design storm return period determines the flood protection level provided by the system (Butler and Davies, 2011). However, such hydraulic reliability-based design approaches place significant emphasis on *identifying* and *quantifying* the probability of occurrence of extreme rainfall and *minimising* the probability of the resulting hydraulic failures i.e. *the fail-safe approach* (Ryu and Butler, 2008; Thorndahl and Willems, 2008). However, such approaches fail to consider other causes of failure for example structural or component failures (Table 1) which also lead to flooding (e.g. Kellagher et al., 2009; Mugume et al., 2014; Ten Veldhuis, 2010).

**Table 1:** Failure modes in urban drainage systems

| Failure mode | Description | Examples/Causes |
|---|---|---|
| Functional failure | Hydraulic overloading due to changes in inflows leading to failure e.g. overflow operation, surcharging and surface flooding | Increase in dry weather flows, extreme rainfall events, excessive infiltration |
| Structural failure | Malfunctioning of single or multiple components in the system such as pumps, tanks or pipes leading to the inability of the failed component to deliver its desired function in full or in part | Pipe collapse, blockages, sediment deposition, solid waste, pump failure, rising main failure |

Furthermore, it is argued that the direct application of reliability-based approaches for evaluation of structural failures in UDSs could be insufficient mainly because causes and

mechanisms of failure are largely unknown and difficult to quantify (Ana and Bauwens, 2010; Kellagher et al., 2009; Park et al., 2013; Ten Veldhuis, 2010). It is therefore important to develop new approaches that seek to ensure that UDSs are designed to not only be reliable during *normal* (standard) loading conditions but also to be resilient to *unexpected* (exceptional) conditions i.e. *the safe-fail approach* (e.g. Butler et al., 2014; Mugume et al., 2014). In this study, the definition and interpretation of resilience in engineering systems is pursued. Resilience is formally defined based on recent work on 'Safe and SuRe' Water Management as the "*the degree to which the system minimises level of service failure magnitude and duration over its design life when subject to exceptional conditions*" (Butler et al., 2014). Exceptional conditions refer to uncertain threats or disturbances that lead to system failure for example climate change induced extreme rainfall events, sewer collapse or blockage. Based on this definition, the goal of resilience is therefore to maintain acceptable functionality levels (by withstanding service failure) and rapidly recover from failure once it occurs (Butler et al., 2014; Lansey, 2012; Park et al., 2013).

Resilience is further classified into two broad categories: a) *general (attribute-based) resilience* which refers to the state of the system that enables it to limit failure duration and magnitude to *any threat* (i.e. all hazards including unknowns) and b) *specified (performance-based)* resilience which refers to the agreed performance of the system in limiting failure magnitude and duration to a *given (known) threat* (Butler et al., 2014; Scholz et al., 2011). Reliability on the other hand is defined as *the degree to which the system minimises the level of service failure frequency over its design life when subject to standard loading* (Butler et al., 2014). Intuitively, it is argued that reliability and resilience are related with the latter extending and building on the former. It is consequently postulated that if resilience builds on reliability, by improving the former, the latter can also be improved (Butler et al., 2014).

Taking the UK water sector as an example, recent studies have proposed range of strategies or options for building resilience in UDSs (Cabinet Office, 2011; CIRIA, 2014; Mcbain et al., 2010). These strategies generally seek to enhance inbuilt system properties or attributes such as *redundancy* and *flexibility* during design, retrofit or rehabilitation so as to influence the ability of the system to withstand the level of service failure and to rapidly recover from failure once it occurs (Hassler and Kohler, 2014; Vugrin et al., 2011). Redundancy is defined as the degree of overlapping function in a system that permits the system to change in order to allow vital functions to continue while formerly redundant elements take on new functions (Hassler and Kohler, 2014). In UDSs, redundancy is enhanced by introducing multiple elements (components) providing similar functions for example storage tanks or parallel pipes, in order to minimize failure propagation through the system or to enable operations to be diverted to alternative parts of the system during exceptional loading conditions (Cabinet Office, 2011; Mugume et al., 2014). Flexibility on the other hand is defined as the inbuilt system capability to adjust or reconfigure so as to maintain acceptable performance levels when subject to multiple (varying) loading conditions (Gersonius et al., 2013; Vugrin et al., 2011). It can be achieved in UDSs, for example, by designing in future proofing options (Gersonius et al., 2013), use of distributed (decentralized) or modular elements for example distributed storage tanks, rainwater harvesting systems, roof disconnection and use of designed multifunctional urban spaces such as car parks, playgrounds or roads (Mugume et al., 2014).

However, the operationalisation of resilience in urban drainage and flood management is still constrained by lack of guidelines, standards, and suitable quantitative evaluation methods (Butler et al., 2014; Ofwat, 2012; Park et al., 2013). In water distribution systems, a number of recent studies have investigated both *component (structural)* and *hydraulic* reliability when subject to stresses such as demand variations, single pipe failure and changes in pipe

roughness (Atkinson et al., 2014; Trifunovic, 2012). In urban drainage systems however, most quantitative studies tend to focus on investigating *hydraulic reliability* which only considers *functional failures* such as occurrence of extreme rainfall or increasing dry weather flows (Sun et al., 2011; Thorndahl and Willems, 2008). The main short coming of such approaches is that the full system failure scenario space that includes other causes of surface flooding such as equipment failure, sewer collapse and blockage is not explored.

It is recognised that different threats or combinations of threats such as extreme rainfall or sewer failure could lead to the same failed state (i.e. surface flooding). Therefore, by only considering a narrow range of hydraulic failures, current approaches take a limited view of *functional resilience* with no due consideration given to *structural resilience*. Further research is needed to develop new quantitative approaches that explicitly consider all possible failure scenarios in order to holistically evaluate resilience in UDSs (Butler et al., 2014; Kellagher et al., 2009; Ofwat, 2012; Ten Veldhuis, 2010).

In this study, a new global resilience analysis approach is developed, that shifts the object of analysis from the threats themselves to explicit consideration of system performance (i.e. failed states) when subject to large number of failure scenarios (Johansson, 2010). Global resilience analysis has been carried out by evaluating the effect of a wide range of progressive structural failure scenarios in various systems such as water distribution systems and electrical power systems (Johansson, 2010). The global resilience analysis (GRA) methodology is extended to investigate the effect of random cumulative link (sewer) failure scenarios on the performance of an UDS. The methodology is then applied to test the effect of implementing two potential adaptation strategies that is; introducing a large centralised detention pond or use of spatially distributed storage tanks) on minimizing loss of functionality during the considered structural failure scenarios.

The key strengths of the developed GRA method is that emphasis is shifted from accurate quantification of the probability of occurrence of sewer failures (e.g. Egger et al., 2013), to evaluating the effect of different sewer failures modes and extent, irrespective of their occurrence probability, on the ability of an UDS to minimise the resulting flooding impacts (e.g. Kellagher et al., 2009).

Link failure envelopes, which show the upper and lower limits (bounds) of the resulting loss of functionality for each considered link failure level are determined based on the hydraulic simulation results from 49,200 scenarios. The failure envelopes reflect vital system resilience properties that determine the resulting loss of functionality when the system is subjected to increasing failure levels. Finally, a new resilience index, $Res_o$ that quantifies system residual functionality as a function of failure magnitude and duration is computed at each failure level for both the existing system and for the tested adaptation strategies.

## 2. Methods

### 2.1 Global resilience analysis (GRA) approach

Global resilience analysis is applied to characterise the performance of an existing UDS when subject to a wide range of structural failure scenarios involving random cumulative link failure. Structural failure in an UDS can be modelled by removal of components for example sewers (links), storage tanks or pumps in the system to represent the inability of the removed component to deliver its prescribed function. In this study, links in an UDS are randomly and cumulatively failed and the resulting impacts on the global performance of the system are investigated for each failure level, until all the links in the system have been failed. This process of cumulative link failure is used to represent structural failure modes such as sewer collapse, blockages and sediment deposition in closed systems and blockage resulting from deposition of solid waste and washed-in sediments in open channel systems. The approach of

failing links randomly ensures that all links, *N* in the system have an equal probability of being removed (Johansson and Hassel, 2012). In addition, a step by step increase in sewer failure levels enables the exploration of the full sewer failure scenario space that ranges from *predictable* or commonly occurring failure scenarios such as single component (*N-1*), or two component (*N-2*) failure modes but also other *unexpected* scenarios involving simultaneous failure of a large number of components (e.g. Johansson, 2010; Park et al., 2013).

To fully explore the extent of the failure scenario space in global resilience analysis, a very large number of model of simulations involving different failure scenarios would be required to capture the resulting flooding impacts (e.g. Kellagher et al., 2009). In addition, different possible sewer (link) states for example non-failed (good condition), partial or complete failure need to be evaluated (Ana and Bauwens, 2010; Kellagher et al., 2009). Taking an UDS with 81 links as an example, and assuming only two link states (non-failed or completely failed), the total number of link failure scenarios within the full failure scenario space would be $2.4 \times 10^{24}$. To reduce the computational time, a convergence analysis (e.g. Trelea, 2003) is carried out to determine the minimum number of random cumulative link failure sequences, $rs_x$ that are required to achieve consistent results (refer to Supplementary information section 1.1). Given the significant computational burden of GRA, a simple 1D approach to modelling of surface flooding (of the minor system) is proposed rather than using more complex 2D overland flow models (Digman et al., 2014; Maksimović et al., 2009).

## 2.2 GRA implementation

The GRA method is implemented in the MATLAB environment linked to the Storm Water Management Model, SWMMv.5.1; a physically based discrete time hydrological and hydraulic model that can be used for single event and continuous simulation of run-off quantity and quality, primarily built for urban areas (Rossman, 2010). Link failure can be modelled in SWMM v5.1 by either significantly reducing pipe diameters in the model (e.g.

Mugume et al., 2014a) or increasing the Manning's roughness coefficient, *n* to a very high value. In this study, link failure is modelled by increasing the Manning's *n from its initial (non-failed) state value* (*n = 0.020*) to a very high value (*n = 100*). The high value of *n* was chosen because it significantly curtails the conveyance of flows in each failed link and hence enables modelling of *complete failure* of each link.

Model simulations are carried out at each randomly generated link failure level and system performance is quantified using the total flood volume and mean duration of nodal flooding as key performance indicators. Surface flooding is simply modelled using the ponding option inbuilt in SWMM which allows exceedance flows to be stored atop of the nodes and to subsequently re-enter the UDS when the capacity allows (Rossman, 2010). The flooding extent at each node is modelled using an assumed ponded area of 7,500 $m^2$. Figure 1 further illustrates the adopted modelling framework. The main steps in implementing the GRA include:

a) A simulation is run to assess UDS performance in its initial (non-failed) state using the considered extreme rainfall loading
b) A randomly selected single link $c_i$ *: i = 1, 2, 3,…N*, in the UDS is failed and a simulation is run using the same extreme rainfall loading. This step represents single link failure mode and is denoted as *N-1*.
c) Two randomly selected links, in the UDS are failed (denoted as *N-2 failure mode*) and the simulation is repeated
d) The procedure is repeated for all *N-i*: *i = 1, 2, 3,…N* failure modes until all the links in the system have been failed.
e) The procedure in (a) – (d) is repeated to determine the minimum number of random failure sequences $rs_x$ that ensures *convergence* of results. A detailed description of

convergence analysis in GRA is presented in the Supplementary information section 1.1).

f) Using the determined $rs_x$, the procedure in (a) – (d) above is repeated to investigate the effect of the proposed adaptation strategies on minimising the loss of system functionality resulting from the considered cumulative link failure scenarios.

## 2.3 Determination of link failure envelopes

The use of average values in reliability and resilience analysis simplifies results interpretation but can potentially hide key information about the range of possible failure impacts and consequences (e.g. Trifunovic, 2012). The process of determining failure envelopes provides a means of graphically illustrating the range of failure impacts at each considered failure level (e.g. Church and Scaparra, 2007). In this study, link failure envelopes are determined by computing the minimum and maximum values of all model solutions (total flood volume and mean duration of nodal flooding) obtained at each considered link failure level for the existing UDS and for the considered adaptation strategies. The resulting envelopes represent the upper and lower limits of the resulting loss of system functionality (impacts) that therefore provide vital information about the resilience properties of the system being tested. If the resulting envelope covers solutions with lower impacts at all link failure levels, then the resulting loss of system functionality is minimised during the considered failure scenarios. If the resulting envelope covers solutions with higher impacts and with a larger range between the minimum and maximum values, the tested system exhibits higher loss of system functionality during the considered failure scenarios (e.g. O'Kelly and Kim, 2007).

## 2.4 Computation of the flood resilience index

The resilience index, $Res_o$, is used to link the resulting loss of functionality to the system's residual functionality and hence the level of resilience at each link failure level. The resulting loss of system functionality is estimated using the concept of *severity*, $Sev_i$ (Hwang et al.,

2015; Lansey, 2012). Severity is interpreted as a function of maximum failure magnitude (peak severity) and failure duration (Figure 2). Figure 2 illustrates the theoretical response of an UDS (in which one or more links have been failed) to a single extreme rainfall loading scenario. In Figure 2, severity can be estimated as the (shaded) area between the original system performance level, $P_o$ and the actual system performance curve, $P_i(t)$, at any time $t$ after occurrence of a given threat that lead to system failure (Equation 1).

$$Sev_i = f\left[Sev_p,\ t_f\right] = \frac{1}{P_o}\int_{t_o}^{t_n}(P_o - P_i(t))dt \quad (1)$$

Where $t_f$ is the failure duration, $t_o$ the time of occurrence of the threat, and $t_n$ the total elapse time. Equation 1 above is further simplified by assuming that the system failure and recovery curve is rectangular (Equation 2)

$$Sev_i = \frac{V_{TF}}{V_{TI}} \times \frac{t_r - t_{fs}}{t_n - t_o} = \frac{V_{TF}}{V_{TI}} \times \frac{t_f}{t_n} \quad (2)$$

The resilience index, $Res_o$, which is a measure of system residual functionality, is estimated as one minus the computed volumetric severity and is computed at each link failure level (Equation 3).

$$Res_o = 1 - Sev_i = 1 - \frac{V_{TF}}{V_{TI}} \times \frac{t_f}{t_n} \quad (3)$$

Where $V_{TF}$ is the total flood volume, $V_{TI}$ the total inflow into the system, $t_f$ the mean duration of nodal flooding and $t_n$ the total elapsed (simulation) time.

For a given threat (i.e. percentage of failed links), the proposed index quantifies the residual functionality of the UDS as function of both the failure magnitude (total flood volume) and duration (mean nodal flood duration). $Res_o$ ranges from 0 to 1; with 0 indicating the lowest level of resilience and 1 the highest level resilience to the considered link failure scenarios. Resilience envelopes are then derived by plotting the minimum and maximum values of $Res_o$ computed at each failure against the percentage of failed links. The resulting envelopes

263 graphically illustrate the system residual functionality at each considered link failure level. A
264 detailed description the theoretical behaviour of an UDS during failure conditions and the
265 derivation of the $Res_o$ is provided in Supplementary information section 1.3.

## 3. Urban drainage system description and modelling results

### 266 3.1 Case study UDS

267 A case study of the existing urban drainage system in the Nakivubo catchment, a highly
268 urbanized part of Kampala city, Uganda is used in this work. The system requires
269 rehabilitation to minimize the frequency, magnitude and duration of flooding during extreme
270 convective rainfall events (Sliuzas et al., 2013). A model of the existing system is built in
271 SWMMv5.1. The full dynamic wave model in SWMM is used to route flows through the
272 modelled UDS. The data needed to build the model has been obtained from a Digital
273 Elevation Model (DEM) for Kampala (2 m horizontal resolution), a 2011 satellite image for
274 Kampala (0.5m horizontal resolution), as-built drawings and from existing reports (e.g.
275 KCC, 2002). A single, non-areally adjusted extreme event was used to represent a worst
276 functional loading case in the GRA. This event used was recorded on 25$^{th}$ June 2012 at 10
277 minute resolution with a 100 minute duration and depth of 66.2 mm (Sliuzas et al., 2013).

278 The existing primary and secondary conveyance system consists of trapezoidal open channel
279 sections constructed using reinforced concrete in upstream sections and gabion walls in the
280 downstream sections. The resulting hydraulic model of the system consists of 81 links, 81
281 nodes and 1 outfall, and with a total conduit length of 22,782 m. The system drains into the
282 Nakivubo wetland and finally into Lake Victoria. The gradients of the open channel sections
283 range from 0.001 to 0.0124. The modelled system drains a total area of 2,793 hectares
284 delineated into 31 sub-catchments (Figure 3**Error! Reference source not found.**). The
285 computed average sub catchment slopes and percentage imperviousness range from 0.034 –

286 0.172 (Figure A.1) and 52.3 – 85.7 (Table A.1) respectively. The existing system is not
287 always clean in a 'business as usual' case. This was reflected in the SWMM model by taking
288 the initial value of *Manning's n* as 0.020 which is the upper limit of the recommended range
289 (i.e. 0.010 – 0.020) for concrete lined channels.

290 **3.2 Modelling the effect of adaptation strategies on UDS performance**

291 Enhancing the resilience of an UDS during design or retrofit can be achieved by altering its
292 configuration in order to enhance its redundancy and flexibility. ***Redundancy*** could be
293 increased by introducing extra elements such additional storage tanks, temporary storage
294 areas or increasing spare capacity in critical links (Butler and Davies, 2011; Cabinet Office,
295 2011; CIRIA, 2014). ***Flexibility*** on the other hand can be increased, for example, by
296 designing in future proofing options, use of distributed elements and provision of back-up
297 capacity (e.g. Gersonius et al., 2013). In this study, two adaptation strategies are modelled
298 tested using the GRA methodology namely, addition of one large centralised detention pond
299 (*centralised storage strategy*) and several, spatially distributed storage tanks (*distributed*
300 *storage strategy*) respectively (Figure A.2).

301 In the *centralised storage* (CS) strategy**,** a large centralised detention pond with a total
302 storage volume of 3.15 x$10^5$ $m^3$ is introduced upstream of link C47 (Figure A.2a) to enhance
303 system redundancy. In choosing the possible location of the centralised storage tank, two
304 main criteria were used; land availability and flow rates in the downstream links in the
305 primary Nakivubo channel. In the *distributed storage (DS) strategy,* 28 spatially distributed
306 upstream storage tanks with a combined total storage volume of 3.15 x $10^5$ $m^3$ are introduced
307 at the outlets of the sub catchments to enhance flexibility in crucial points in the network
308 (Figure A.2b). The DS strategy models upstream distributed source control.

309

### 3.3 Simulation and performance assessment of the existing UDS

In order to test the performance of the modelled existing UDS, simulations were carried out and flows were investigated at selected links in the system (Figure 4). The hydraulic data on the selected open channel cross sections is presented in Table A.2.

Lower peak flow rates, are simulated in most upstream links. The flow rates increase along the system leading to very high peaks in downstream links, for example flows of 297.4 $m^3/s$ and 318.2 $m^3/s$ are simulated at downstream links C76 and C81 respectively after an elapsed time of 75 minutes (Figure A.3). Globally, 57 links (70.4%) in the system experience hydraulic overloading that consequently leads to surface flooding. Hydraulic overloading in links occurs when: (i) the upstream ends of the link run at full capacity and (ii) when the slope of the hydraulic grade line exceeds the slope of the link (Butler and Davies, 2011). The most severe hydraulic overloading is simulated in 26 links (32%), with the duration of hydraulic overloading ranging from 13 – 54 minutes.

The results of the simulation also indicate the system experiences flooding at a total of 57 nodes, representing a flood extent of 70.7%, with a total volume of flooding of 706, 045 $m^3$ and mean nodal flood duration of 48 ± 4 minutes.

### 3.4 Global resilience analysis of the existing UDS

The proposed GRA methodology described in section 2 is applied to characterise the performance of existing UDS. The overall performance of the system is quantified by simulating total flood volume and mean duration of flooding resulting from 16,400 link failure scenarios generated from 200 random link failure sequences (Figure A.4). The average values of the total flood volume and duration of nodal flooding are computed for all the considered link failure scenarios and are presented in Figure 5. The GRA results indicate that failure of just 10% of links leads to a disproportionately large increase of 91% in total

flood volume (Figure 5a). Thereafter, further increase in the percentage of failed links leads to comparatively small increases in the total flood volume.

The situation is very different for nodal flood duration, where results show failure of 10% of links leads to just a 6% increase (Figure 5b). Globally, the results indicate that the failure duration increases from 41 minutes to 56 minutes representing an increase of 36.2% when all the links in the system are failed.

### 3.5 Effect of adaptation strategies on system performance

The GRA methodology is applied to test each of the proposed UDS adaptation strategies. An additional 16,400 link failure scenarios are simulated for the CS and DS strategies respectively that is, a total of 32,800 generated from a total of 400 random link failure sequences (Figure A.4). The effect of the CS strategy is a slight reduction of flood volume which occurs at lower link failure levels less than 60% with very little impact on flood duration at all failure levels. Globally, it results in a 3.4% reduction of total flood volume and a 1.1% increase in mean duration of flooding (Figure 5).

On the other hand, the DS strategy results in a significant reduction of 32% total flood volume at all considered link failure levels. At link failure levels greater than 20% any additional increase in link failure levels leads to minimal increase in total flood volume. The strategy also reduces the mean nodal flooding duration from 48 minutes to 35 minutes giving a reduction of 27% for all considered link failure scenarios. Table 3 details the key statistics of the GRA results for the existing system and for the considered resilience strategies.

**Table 2:** Mean values of GRA analysis results for all considered link failure scenarios. The values in the square brackets indicate the reduction range computed by considering 1 standard deviation of the mean.

| Strategy | Flood volume (x10$^3$ m$^3$) | | | Mean nodal flood duration (hrs) | | |
|---|---|---|---|---|---|---|
| | Mean, μ | Standard deviation, σ | % reduction | Mean, μ | Standard deviation, σ | % reduction |
| Existing system | 1,457.5 | 143.6 | | 0.80 | 0.07 | |
| Centralised storage | 1,408.8 | 183.4 | 3.3 [1.0 - 5.1] | 0.81 | 0.07 | -1.1 [-2.3 - -0.2] |
| Distributed storage | 986.1 | 96.3 | 32.3 [29.9 - 34.1] | 0.59 | 0.03 | 26.8 [25.6 - 28.4] |

### 3.6 Link failure envelopes

The resulting link failure envelopes which represent the range of model solutions from the lowest to the highest flooding impacts computed at each link failure level are presented in Figure 6. For the existing UDS and considering the flood volume, a large range of deviation between the computed failure envelopes and the mean values (27 – 87%) is observed at lower link failure levels (<20%). A convergence of both failure envelopes is observed at higher link failure levels. The results from the nodal flood duration are different, and indicate a narrow range of deviation (< 26.3%) between resulting failure envelopes and the mean values at all link failure levels. Rather similar ranges of deviation between the resulting flood volume and flood duration failure envelopes and the respective mean values are observed for the CS and DS strategies respectively.

In order to evaluate the effectiveness of the considered adaptation strategies, the generated link failure envelopes are plotted into one graph to map out the failure space common to all (Figure 7). Comparing the results of the CS strategy to those of the existing system, a slight downward shift of both the maximum and minimum flood volume failure envelopes is observed at lower link failure levels (< 40%), which represents the effect of the strategy in minimising the magnitude of flooding. However, there is no significant effect at higher link

failure levels. Also, the results suggest that the CS strategy has minimal effect on the flood duration failure envelopes.

For the DS strategy, a significant downward shift in the flood volume failure envelope (i.e. a reduction in the magnitude of flooding) is observed link failure envelope at all cumulative link failure levels. The strategy also limits the additional increase in flood volume for link failure levels beyond 33% i.e. a flattening of the flood volume failure envelope is observed at higher link failure levels. The strategy also shifts the flood duration failure envelopes downwards (i.e. reduces the failure duration) for all considered link failure levels when compared the existing UDS.

### 3.7 Resilience index

The resilience index ($Res_o$) is computed using Equation 3, for all simulated link failure scenarios. Based on the computed indices, resilience envelopes which represent the residual functionality of the whole UDS as a function of both the failure magnitude and duration are determined by computing the minimum and maximum values of $Res_o$ at each link failure level for the existing system for the tested adaptation strategies (Figure 8). To facilitate comparison of the performance of the tested strategies, an assumed acceptable level of resilience threshold of 0.7 is plotted on each of the graphs, as an example of the minimum acceptable flood protection level of service (for example no property flooding) that needs to be achieved by the considered adaptation strategies.

The figure reveals large variations in $Res_o$ for the existing system and for the tested strategies at lower link failure levels (< 20%) with a convergence of the results occurring with increasing link failure levels. For the existing UDS, the computed mean values of $Res_o$ range from 0.54 to 0.66. When compared to the resilience threshold, the results indicate that the existing system crosses this threshold when link failure levels in system exceed 6.2%.

Considering the CS strategy, a slight improvement in $Res_o$ of 1.2 - 2.3% is observed. The results indicate that resilience index falls below the threshold value when link failure levels exceed 8.6%. When the distributed storage strategy is considered, higher mean values of $Res_o$ are computed (0.76 – 0.84). The results also indicate that for the DS strategy, the resilience threshold is not crossed at all link failure levels. Overall, the DS strategy leads to significant improvement in the $Res_o$ of 27.5 – 41.4%.

## 4. Discussion of results

### 4.1 Existing system

Considering the existing system, random failure of less than 20% of the links leads to disproportionately high degradation of system functionality magnitude (i.e. total flood volume). The disproportionately high loss of system functionality suggests that failure of a small fraction of links rapidly reduces the global hydraulic conveyance capacity of the (minor) system. This result is also confirmed by critical component analysis (e.g. Johansson and Hassel, 2012) involving targeted failure of single (individual) links in the UDS (Refer to supplementary information section 1.1, Figure S2) This therefore suggests that the existing UDS exhibits low levels of resilience to sewer failures. This could be attributed to the already insufficient hydraulic capacity of the system (due to use of an extreme rainstorm for modelling purposes) but could also be attributed to other key factors such as its dendritic network topology and limitations of using 1D modelling approach which excludes the contribution of the major system (i.e. effect of additional redundancies) in conveying surface flows to downstream parts of the system during extreme events.

In contrast to the total flood volume, random cumulative link failure has a limited effect on mean nodal flood duration. This could be attributed to use of a single short duration rainfall event for the simulations as opposed to using multiple events. Similarly, this could also be attributed limitations of using a simplified above ground flood model. By using a simplified

425 above-ground flood model, surface flooding which occurs in the major system (i.e. overland
426 flood pathways such as roads, paths or grass ways) during extreme events and which may
427 also cause substantial damage to property and infrastructure is not considered, which could
428 also lead to inaccurate estimation of the mean flood duration (e.g. Digman et al., 2014;
429 Maksimović et al., 2009).

430 **4.2 Effect of adaptation strategies**

431 It is argued that an effective adaptation strategy should result in a downward shift (i.e.
432 towards the origin) of the failure envelope of the existing system. By doing this, the failure
433 magnitude and duration is minimised across the considered failure scenarios. The derived
434 link failure envelopes suggest that CS strategy has a very limited effect on minimising the
435 total flood volume, with the reduction being achieved at lower link failure levels. More so, no
436 significant effect on flood duration at all considered link failure levels. As a consequence, the
437 CS strategy only minimally improves the residual functionality of the existing system during
438 the considered link failure scenarios. This therefore suggests that sewer failures could
439 significantly limit the effectiveness of adaptation strategies involving enhancement of
440 redundancy at a single location in the UDS. This also suggests that other preventive asset
441 management strategies for example improved cleaning and maintenance practices may be
442 more effective for resilience enhancement, because they in increase spare capacity in the
443 links themselves and minimise structural failure in existing systems (e.g. Ten Veldhuis, 2010)

444 In contrast the CS strategy, the study results suggest that the DS strategy is more effective in
445 minimising the resulting loss of functionality at all link failure levels. This could be attributed
446 to the effect of increased the spatial distribution of control strategies (i.e. smaller
447 decentralised upstream storage tanks with the same total storage volume as the CS strategy)
448 results in optimal use of the total storage volume for reduction both the storm water volume
449 and the inflow rates before entry into UDS. Reducing the stormwater inflows into the system

in turn enables the degraded UDS to continue functioning with minimal impacts. It could also be due to a reduction in propagation of hydraulic failures from one part of the UDS to another, which suggests that the DS strategy improves the flexibility properties of the whole (minor) system. Using this argument, it could be suggested that adaptation strategies that increase the spatial distribution of control strategies in upstream parts of the catchment for example implementation of multifunctional (dual-purpose) rainwater harvesting (DeBusk, 2013) at a city district or catchment scale could significantly increase the resilience UDSs to sewer failures.

### 4.3 Outlook

The developed global resilience analysis approach presents a promising quantitative tool which opens up new opportunities for holistic and systematic evaluation of the effect of a wide range of threats that have not been considered in conventional hydraulic reliability based urban drainage design and rehabilitation approaches. Future research will compare the results obtained by the presented GRA method with those obtained by using dual-drainage (1D-1D) or 2D rapid flood spreading models (e.g. Blanc et al., 2012; Maksimović et al., 2009) in GRA to account for the effect of the major system in providing additional system redundancies during flooding conditions.

Additionally, the following areas are recommended for further research.

- Investigation of the influence of inherent/inbuilt UDS characteristics for example network structure, network size (number of links), pipe diameters, pipe gradients on resilience to structural failures.
- Investigation of the effect of other types of component failures (e.g. pump failures) on global resilience in UDSs.

- Investigation of the linkages and interdependences between UDS failure (flooding) and unexpected failures in interconnected systems such as electrical power systems.
- Further investigation aimed at linking the computed resilience indices to new resilience-based flood protection level of service standards that are based on minimisation of the magnitude and duration flooding as opposed to use of design return periods.

## 5. Conclusions

This research has tested and extended the global resilience analysis (GRA) methodology to systematically evaluate UDS system resilience to random cumulative link (sewer) failure. The GRA method presents a new and promising approach for performance evaluation of UDSs that shifts emphasis from prediction of the probability of occurrence of key threats that lead to flooding (fail-safe approach) to evaluating the effects of a wide range of failure scenarios that not only includes functional failures but also structural or component failures which also contribute to flooding in cities.

In this study, the effect of a wide range of random and progressive sewer (link) failure scenarios on the ability of existing and adapted UDSs to minimise the resulting loss of functionality has been investigated. Link failure envelopes have been determined by computing the minimum and maximum values of the total flood volume and mean nodal flood duration results generated by simulating a large number of random cumulative link failure scenarios. A new resilience index has been developed and used to link the resulting loss of functionality to the system's residual functionality at each link failure level. Based on the results of the study, the following conclusions are drawn.

- The presented global resilience analysis approach provides a promising quantitative evaluation tool that enables consideration of wide range of possible sewer failure scenarios ranging from *normal* to *unexpected* with reduced computational complexity.

497 - The use of convergence analysis enables determination of the minimum number of
498 random cumulative link failure sequences require to achieve consistent GRA results,
499 which in turn enhances that practicability of resilience assessment by significantly
500 reducing the computational complexity involved in simulating all possible sewer
501 failure combinations.
502 - Building resilience in UDSs to unexpected failures necessitates explicit consideration
503 of the contribution of different failure modes, effect of interactions between different
504 failures modes for example interdependences between sewer failures and hydraulic
505 overloading in UDS design or performance evaluation of existing systems.
506 - Building resilience in UDSs should not only be addressed through capital investments
507 aimed at enhancing inherent UDS properties such as redundancy and flexibility but
508 should also consider investments in asset management strategies such as sewer
509 cleaning and maintenance of existing UDSs.

**Acknowledgement**

510 This research is financially supported through a UK Commonwealth PhD scholarship
511 awarded to the first author. The work is also supported through the UK Engineering &
512 Physical Sciences Research Council (ESPRC) funded Safe & SuRe research fellowship
513 (EP/K006924/1) awarded to last author. Acknowledgement is given to the National Water
514 and Sewerage Corporation (NWSC) and the Kampala Capital City Authority (KCCA),
515 Uganda for providing datasets used in SWMM model development. Thanks are given to Dr.
516 Richard Sliuzas (University of Twentwe, Netherlands) for provision of high resolution
517 rainfall data for Kampala. The insights of the three anonymous reviewers are also gratefully
518 acknowledged.

519 **References**


520 Ana, E. V., Bauwens, W., 2010. Modeling the structural deterioration of urban drainage
521 pipes: the state-of-the-art in statistical methods. Urban Water J. 7, 47–59.
522 doi:10.1080/15730620903447597

523 Atkinson, S., Farmani, R., Memon, F.A., Butler, D., 2014. Reliability indicators for water
524 distribution system design: Comparison. Water Resour. Plan. Manag. 140, 160–168.
525 doi:10.1061/(ASCE)WR.1943-5452.0000304.

526 Blackmore, J.M., Plant, R.A.J., 2008. Risk and Resilience to Enhance Sustainability with
527 Application to Urban Water Systems. Water Resour. Plan. Manag. 134, 224 – 233.

528 Blanc, J., Hall, J.W., Roche, N., Dawson, R.J., Cesses, Y., Burton, A., Kilsby, C.G., 2012.
529 Enhanced efficiency of pluvial flood risk estimation in urban areas using spatial –
530 temporal rainfall simulations. Flood risk Manag. 5, 143–152. doi:10.1111/j.1753-
531 318X.2012.01135.x

532 Butler, D., Davies, J.W., 2011. Urban Drainage, 3rd ed. Spon Press, Taylor and Francis
533 Group, London and New York.

534 Butler, D., Farmani, R., Fu, G., Ward, S., Diao, K., Astaraie-Imani, M., 2014. A new
535 approach to urban water management: Safe and SuRe, in: 16th Water Distribution
536 System Analysis Conference, WDSA2014 - Urban Water Hydroinformatics and
537 Strategic Planning. Procedia Engineering, pp. 347–354. doi:doi:
538 10.1016/j.proeng.2014.11.198

539 Cabinet Office, 2011. Keeping the country running: Natural hazards and infrastructure.
540 London.

541 Church, R., Scaparra, P.M., 2007. Analysis of facility systems' reliability when subject to
542 attack or a natural disaster, in: Murray, A.T., Grubesic, T.H. (Eds.), Critical
543 Infrastructure: Reliability and Resilience. Springer-Verlag Berlin Heidelberg, pp. 221–
544 241.

545 CIRIA, 2014. Managing urban flooding from heavy rainfall - encouraging the uptake of
546 designing for exceedance. London.

547 DeBusk, K.M., 2013. Rainwater Harvesting: Integrating Water Conservation and Stormwater
548 Management. North Carolina State University, Raleigh, North Carolina.

549 Digman, C.J., Anderson, N., Rhodes, G., Balmforth, D.J., Kenney, S., 2014. Realising the
550 benefits of integrated urban drainage models. Water Manag. 167, 30–37.
551 doi:10.1680/wama.12.00083

552 Djordjević, S., Butler, D., Gourbesville, P., Mark, O., Pasche, E., 2011. New policies to deal
553 with climate change and other drivers impacting on resilience to flooding in urban areas:
554 the CORFU approach. Environ. Sci. Policy 14, 864–873.
555 doi:10.1016/j.envsci.2011.05.008

556 Egger, C., Scheidegger, A., Reichert, P., Maurer, M., 2013. Sewer deterioration modeling
557 with condition data lacking historical records. Water Res. 47, 6762–6779.
558 doi:10.1016/j.watres.2013.09.010

559 Gersonius, B., Ashley, R., Pathirana, A., Zevenbergen, C., 2013. Climate change uncertainty:
560 building flexibility into water and flood risk infrastructure. Clim. Chang. 116, 411–423.
561 doi:10.1007/s10584-012-0494-5

562 Hassler, U., Kohler, N., 2014. Resilience in the built environment. Build. Res. Inf. 42, 119–
563 129. doi:10.1080/09613218.2014.873593

564 Holling, C.S., 1996. Engineering Resilience versus Ecological Resilience, in: Schulze, P.
565 (Ed.), Engineering within Ecological Constraints. National Academy Press, Washington
566 DC, USA, pp. 31–44.

567 Hwang, H., Lansey, K., Quintanar, D.R., 2015. Resilience-based failure mode effects and
568 criticality analysis for regional water supply system. J. Hydroinformatics 17, 193–2010.
569 doi:10.2166/hydro.2014.111

570 IPCC, 2014. Summary for Policy Makers, in: Field, C.B., Barros, V.R., Dokken, D.J., Mach,
571 K.J., Mastrandrea, M.D., Bilir, T.E., Chatterjee, M., Ebi, K.L., Estrada, Y.O., Genova,
572 R.C., Girma, B., Kissel, E.S., Levy, A.N., MacCracken, S., Mastrandrea, P.R., White,
573 L.L. (Eds.), Climate Change 2014: Impacts, Adaptation and Vulnerability -
574 Contributions of the Working Group II to the Fifth Assessment Report. Cambridge
575 University Press, Cambridge and New York, pp. 1–32.

576 Johansson, J., 2010. Risk and Vulnerability Analysis of Interdependent Technical
577 Infrastructures Addressing Socio-Technical Systems. PhD Thesis, Lund University,
578 Lund.

579 Johansson, J., Hassel, H., 2012. Modelling, Simulation and Vulnerability Analysis of
580 Interdependent Technical Infrastructures, in: Hokstad, P., Utne, I.B., Vatn, J. (Eds.),
581 Risk and Interdependencies in Critical Infrastructures - A Guideline for Analysis.
582 Springer, London Heidelberg New York Dordrecht, pp. 49–65.

583 KCC, 2002. Nakivubo channel rehabilitation project, Kampala Drainage Master Plan:
584 Volume 5 - Inventories. Kampala.

585 Kellagher, R.B.B., Cesses, Y., Di Mauro, M., Gouldby, B., 2009. An urban drainage flood
586 risk procedure - a comprehensive approach, in: The WaPUG Annual Conference. HR
587 Wallingford, Blackpool.

588 Lansey, K., 2012. Sustainable, robust, resilient, water distribution systems, in: 14th Water
589 Distribution Systems Analysis Conference. Engineers Australia, pp. 1–18.

590 Maksimović, Č., Prodanović, D., Djordjević, S., Boonya-Aroonnet, S., Leitão, J.P., Allitt, R.,
591 2009. Overland flow and pathway analysis for modelling of urban pluvial flooding.
592 Hydraul. Res. 47, 512–523. doi:10.3826/jhr.2009.3361

Mcbain, W., Wilkes, D., Retter, M., 2010. Flood resilience and resistance for critical infrastructure. London.

Mugume, S.N., Diao, K., Astaraie-Imani, M., Fu, G., Farmani, R., Butler, D., 2014. Building resilience in urban water systems for sustainable cities of the future, in: IWA World Water Congress and Exhibition. IWA, Lisbon, p. 72.

O'Kelly, M.E., Kim, H., 2007. Survivability of commercial backbornes with peering: A case study of Korean networks, in: Murray, A.T., Grubesic, T.H. (Eds.), Critical Infrastructure: Reliability and Resilience. Springer, Berlin, Heidelberg, New York, pp. 107–127.

Ofwat, 2012. Resilience - outcomes focused regulation. Principles for resilience planning. Birmingham.

Park, J., Seager, T.P., Rao, P.S.C., Convertino, M., Linkov, I., 2013. Integrating risk and resilience approaches to catastrophe management in engineering systems. Risk Anal. 33, 356–367. doi:10.1111/j.1539-6924.2012.01885.x

Rossman, L., 2010. Storm Water Management Model - User's Manual Version 5.0. Cincinnati, Ohio.

Ryu, J., Butler, D., 2008. Managing sewer flood risk, in: 11th Int. Conference on Urban Drainage. Edinburgh, Scotland, pp. 1–8.

Scholz, R.W., Blumer, Y.B., Brand, F.S., 2011. Risk, vulnerability, robustness, and resilience from a decision-theoretic perspective. J. Risk Res. 1–18. doi:10.1080/13669877.2011.634522

Sliuzas, R., Jetten, V., Flacke, J., Lwasa, S., Wasige, J., Pettersen, G., 2013. Flood Risk Assessment, Strategies and Actions for Improving Flood Risk Management in Kampala. Kampala.

Sun, S., Djordjević, S., Khu, S., 2011. A general framework for flood risk-based storm sewer network design. Urban Water J. 8, 13–27. doi:10.1080/1573062X.2010.542819

Ten Veldhuis, J.A.E., 2010. Quantitative risk analysis of urban flooding in lowland areas. PhD Thesis, Delft University of Technology.

Thorndahl, S., Willems, P., 2008. Probabilistic modelling of overflow, surcharge and flooding in urban drainage using the first-order reliability method and parameterization of local rain series. Water Res. 42, 455 – 466.

Trelea, I.C., 2003. The particle swarm optimization algorithm: Convergence analysis and parameter selection. Inf. Process. Lett. 85, 317–325. doi:10.1016/S0020-0190(02)00447-7

Trifunovic, N., 2012. Pattern Recognition For Reliability Assessment Of Water Distribution Networks. CRC Press. PhD Thesis, Delft University of Technology.

629 Vugrin, E.D., Warren, D.E., Ehlen, M.A., 2011. A resilience assessment framework for
630 infrastructure and economic systems: Quantitative and qualitative resilience analysis of
631 petrochemical supply chains to a hurricane. Process Saf. Prog. 30. doi:10.1002/prs

632

# Appendix

## Appendix Tables

**Table A.1:** Sub catchment area and computed percentage imperviousness

| Sub catchment ID | Sub catchment area (ha) | Imperviousness (%) |
|---|---|---|
| S1 | 83.6 | 69.9 |
| S2 | 59.5 | 71.3 |
| S3 | 69.0 | 67.2 |
| S4 | 97.2 | 84.1 |
| S5 | 52.0 | 81.1 |
| S6 | 46.1 | 76.6 |
| S7 | 23.8 | 82.7 |
| S8 | 10.2 | 66.2 |
| S9 | 60.0 | 72.4 |
| S10 | 144.4 | 72.0 |
| S11 | 76.1 | 71.5 |
| S12 | 81.4 | 71.1 |
| S13 | 50.0 | 79.6 |
| S14 | 67.3 | 75.3 |
| S15 | 57.4 | 70.7 |
| S16 | 55.4 | 52.3 |
| S17 | 67.9 | 61.5 |
| S18 | 52.9 | 56.6 |
| S19 | 52.3 | 66.7 |
| S20 | 158.8 | 61.5 |
| S21 | 108.5 | 71.6 |
| S22 | 71.0 | 78.2 |
| S23 | 89.1 | 82.1 |
| S24 | 25.4 | 85.7 |
| S25 | 199.9 | 68.1 |
| S26 | 115.7 | 62.7 |
| S27 | 147.5 | 80.7 |
| S28 | 134.4 | 75.8 |
| S29 | 23.1 | 81.1 |
| S30 | 88.7 | 69.1 |
| S31 | 424.4 | 73.0 |
| **Total Area** | **2,793.2** | |

640 **Table A.2:** Hydraulic data of selected trapezoidal open channel sections in the Nakivubo UDS. The slope values
641 represent ratios of horizontal to vertical distance.

| Link | Length (m) | depth, d (m) | bottom width, b (m) | left slope | right slope | Equivalent pipe diameter, $D_e$ (m) |
|---|---|---|---|---|---|---|
| C12 | 100.0 | 1.8 | 4.3 | 0.743 | 0.743 | 3.5 |
| C40 | 290.0 | 2.5 | 1.0 | 1.000 | 1.000 | 3.3 |
| C54 | 512.6 | 1.5 | 1.0 | 0.667 | 0.667 | 2.0 |
| C76 | 400.0 | 4.3 | 17.4 | 0.040 | 0.040 | 9.8 |
| C81 | 400.0 | 2.0 | 26.0 | 1.375 | 1.375 | 8.6 |

642

643 **Table A.3:** Distributed storage tank volumes

| Storage tank ID | Volume ($m^3$) |
|---|---|
| ds1 | 9,433 |
| ds2 | 6,711 |
| ds3 | 7,782 |
| ds4 | 10,956 |
| ds567 | 13,743 |
| ds8 | 1,151 |
| ds9 | 6,770 |
| ds10 | 16,287 |
| ds11 | 8,582 |
| ds12 | 9,181 |
| ds13 | 5,639 |
| ds14 | 7,591 |
| ds16 | 6,243 |
| ds17 | 13,623 |
| ds19 | 5,899 |
| ds20 | 17,906 |
| ds21 | 12,239 |
| ds22 | 8,011 |
| ds23 | 10,052 |
| ds24 | 2,859 |
| ds25 | 22,547 |
| ds26 | 13,051 |
| ds31 | 47,864 |
| ds30 | 10,000 |
| ds29 | 2,609 |
| ds28 | 15,160 |
| ds27 | 16,636 |
| ds15 | 6,474 |

644

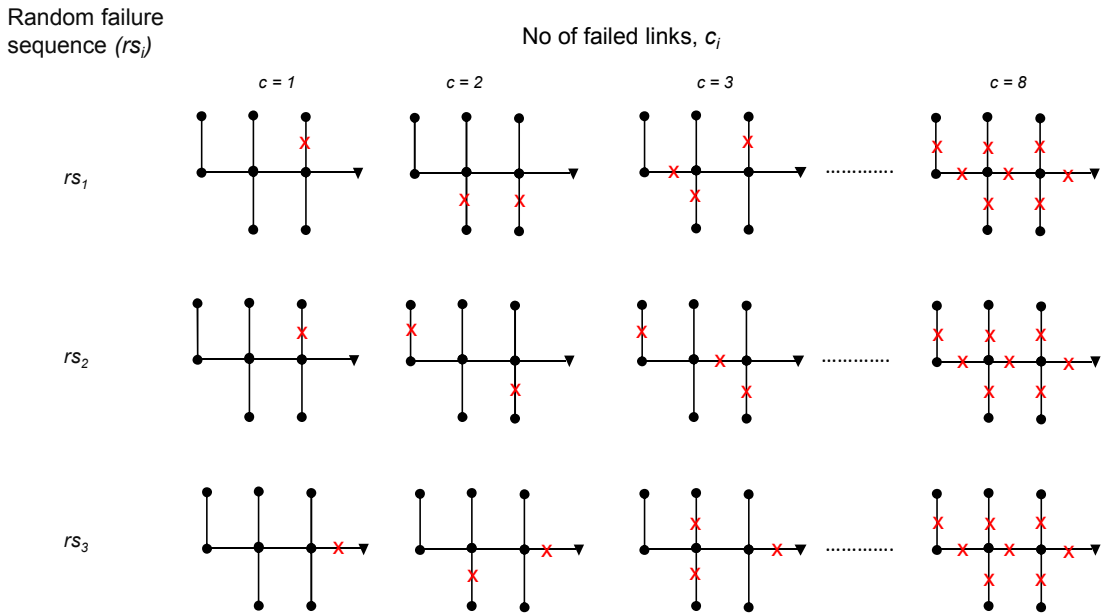


Figure 1: Modelling framework for random cumulative link failure in a simplified urban drainage system with 8 links, 8 nodes and 1 outfall illustrating (a) random and increasing link failure levels $c_1$, $c_2$, $c_3 ... c_N$ and (b) three potential random failure sequences $rs_1$, $rs_2$ *and* $rs_3$

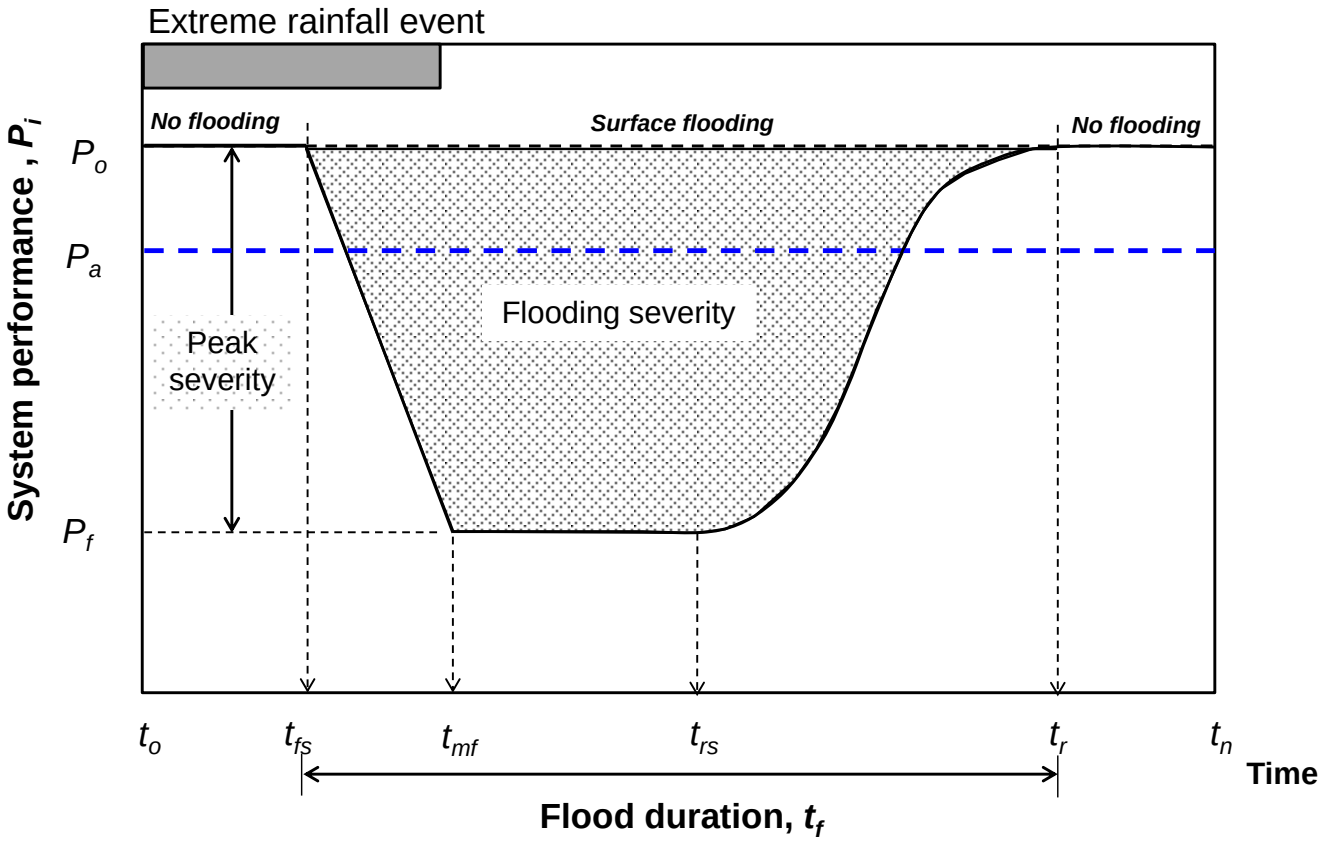


Figure 2: Theoretical system performance curve for an urban drainage system. The block solid line, $P_o$ represents the original (design) performance level of service. The blue dotted line, $P_a$ represents a lower but acceptable level of service. $P_f$ represents the maximum system failure level resulting from the considered threat.

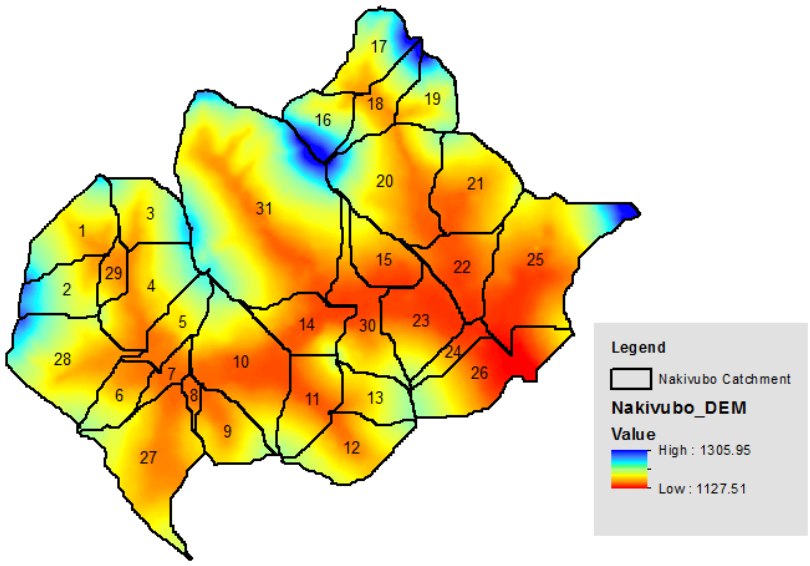


Figure 3: Digital elevation model and delineated sub catchments in the Nakivubo catchment

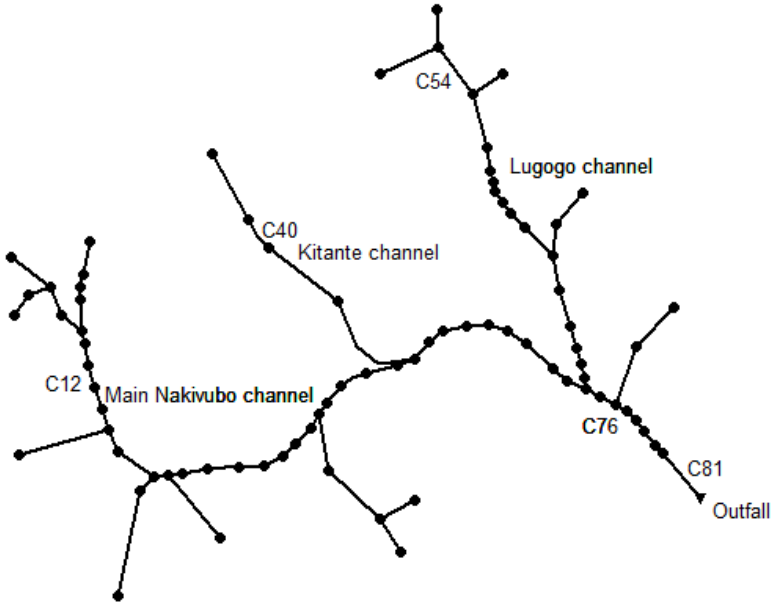


Figure 4: Layout of the modelled Nakivubo urban drainage network

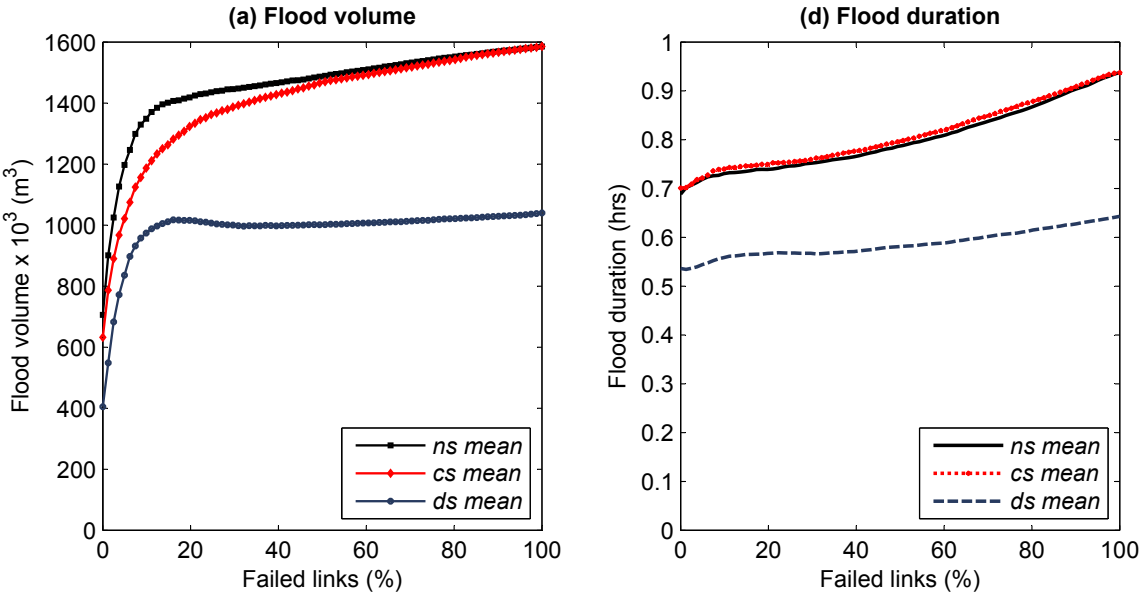


Figure 5: Effect of cumulative link failure on (a) total flood volume (b) mean duration of nodal flooding for the existing UDS *(ns mean)*, for the centralised storage strategy *(cs mean)* and for the distributed storage strategy *(ds mean)*

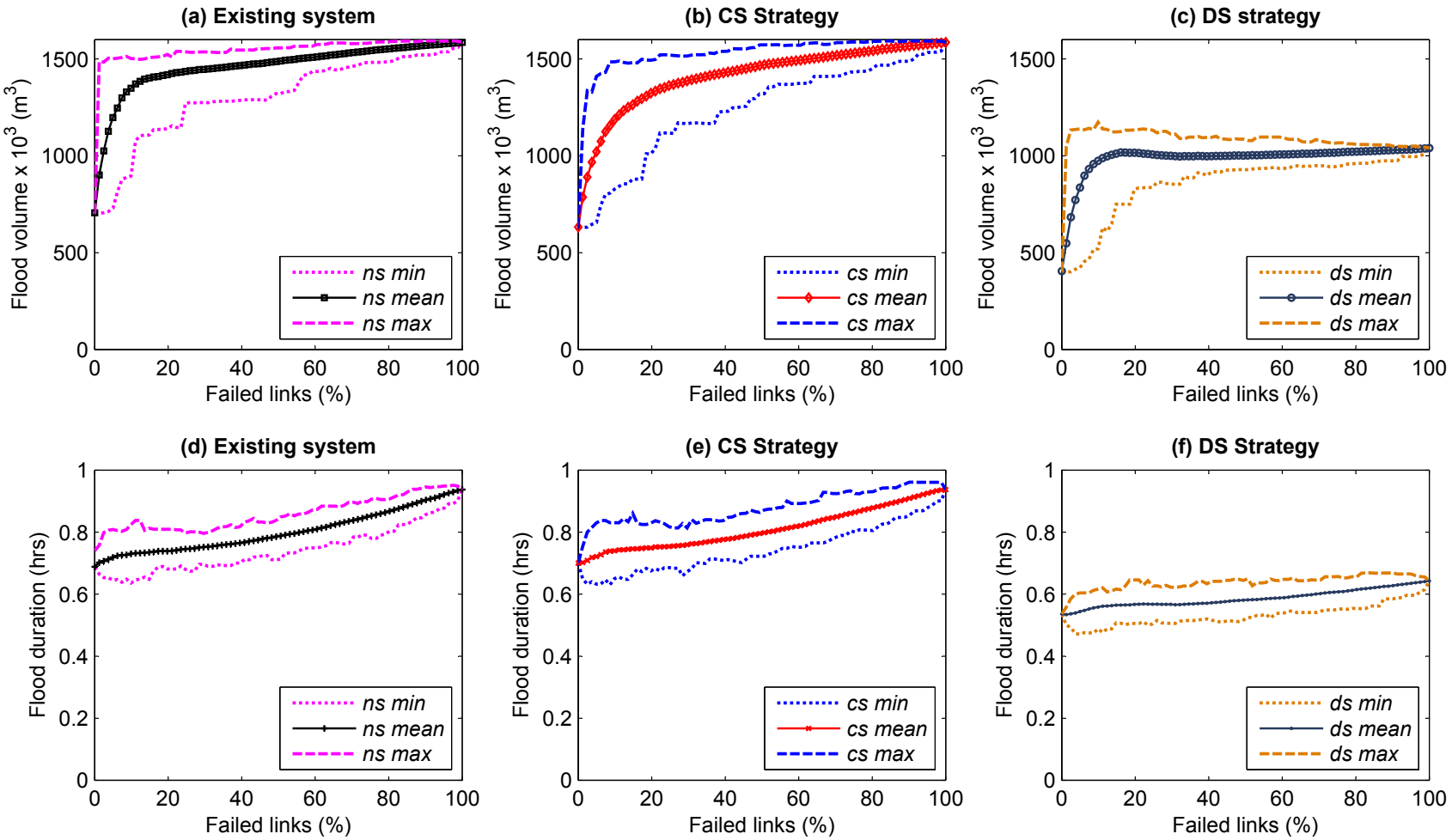


Figure 6: Results of generated link failure envelopes for total flood volume (a) - (c) and for mean duration of nodal flooding (e) - (f) for the existing UDS and for the CS and DS strategies

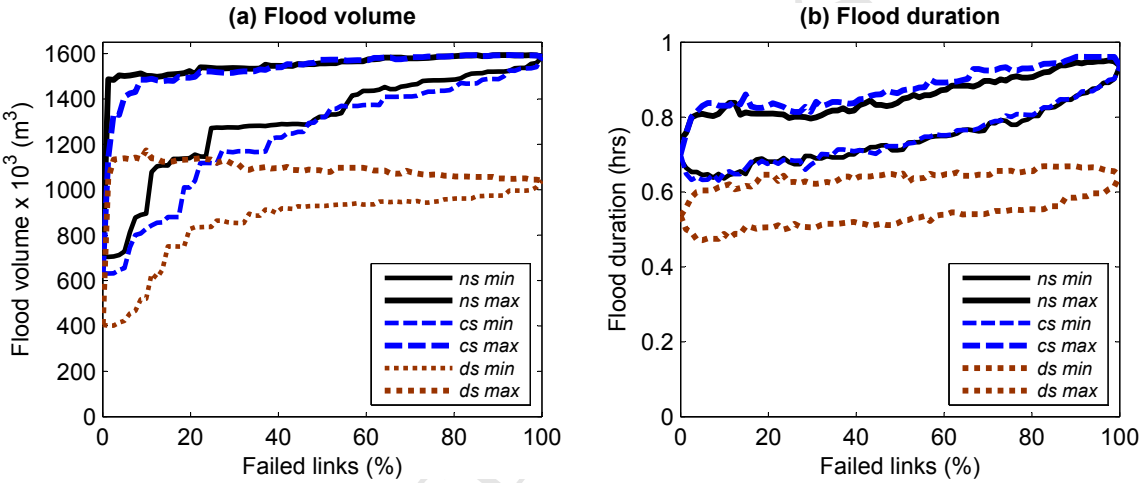


Figure 7: Intersection of cumulative link failure envelopes for the existing system and for the CS and DS strategies

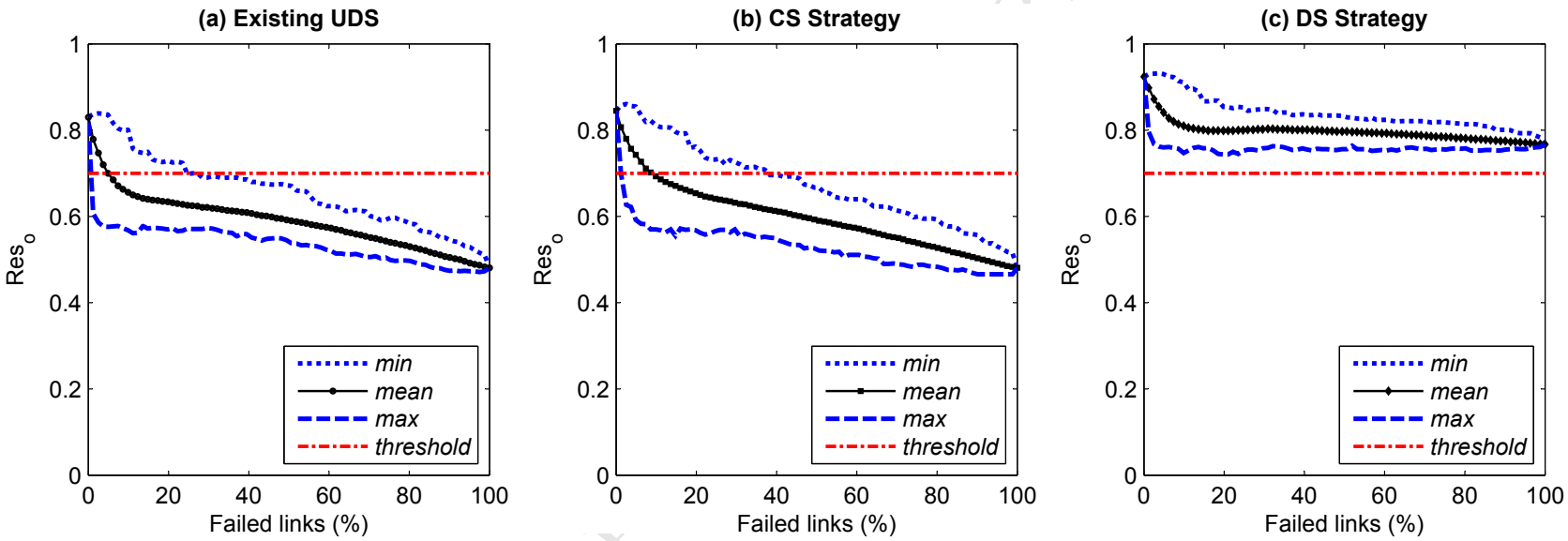


Figure 8: Resilience envelopes showing maximum, mean, minimum values of $Res_o$ computed at each link failure level for (a) existing UDS, (b) CS strategy and (c) DS strategy. The red dashed dot horizontal line is an assumed minimum acceptable resilience level of service threshold of 0.7

**Paper highlights**

- Quantitative evaluation of both hydraulic and structural failures in urban drainage systems.
- Investigation of a wide range of sewer failure scenarios with reduced computational complexity.
- Simulation of 49,200 random structural failure scenarios to determine link failure envelopes.
- Development of a new resilience index for quantifying system residual functionality.
- Effectiveness of adaptation strategies in improving structural resilience tested.

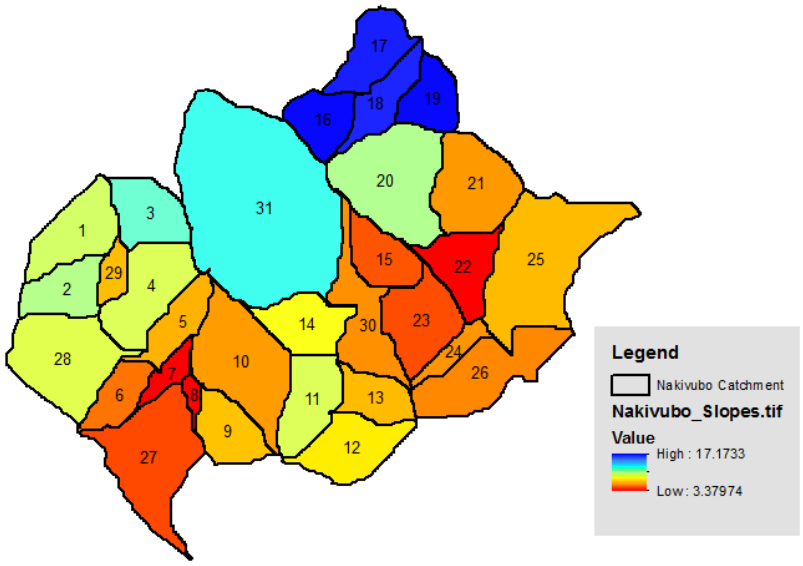


Figure A.1: Computed Nakivubo subcatchment slopes

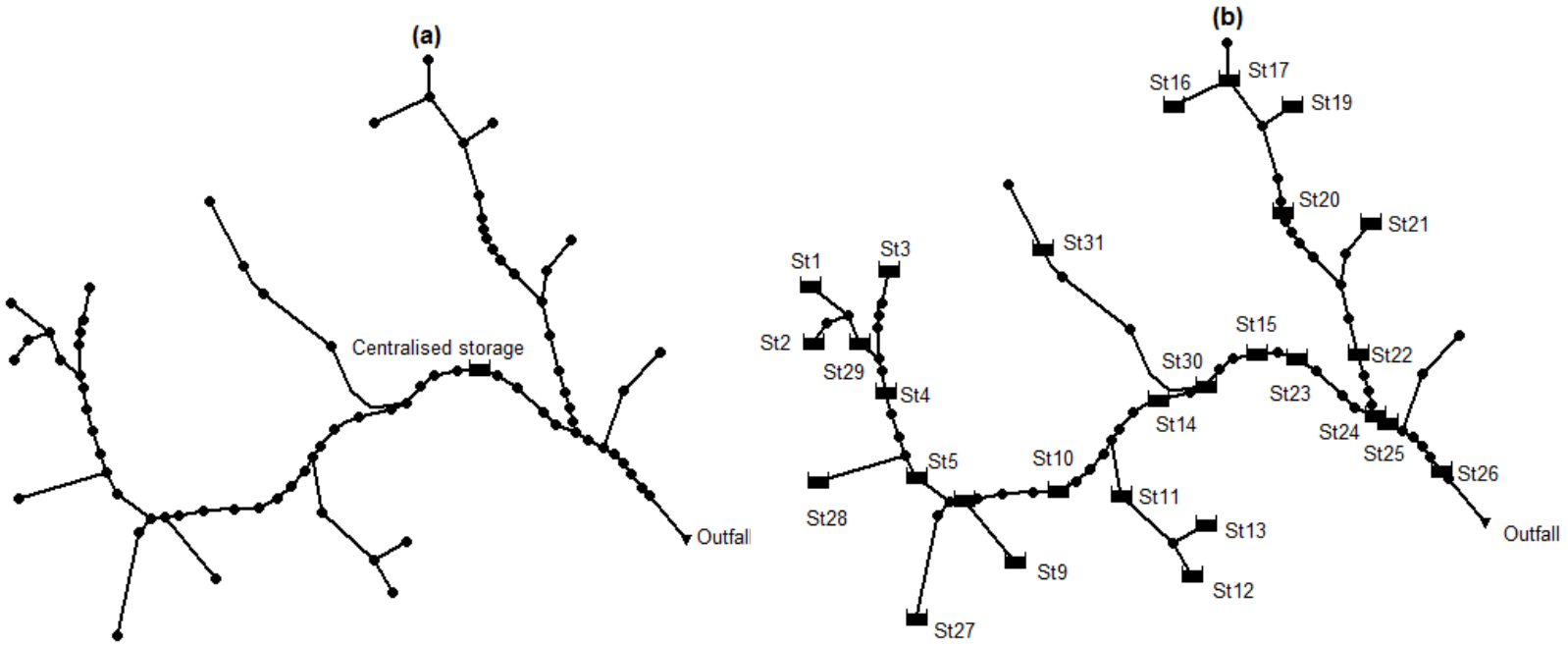


Figure A.2: Layout of adapted UDS (a) centralised storage (CS) and (b) upstream distributed storage (DS) strategy

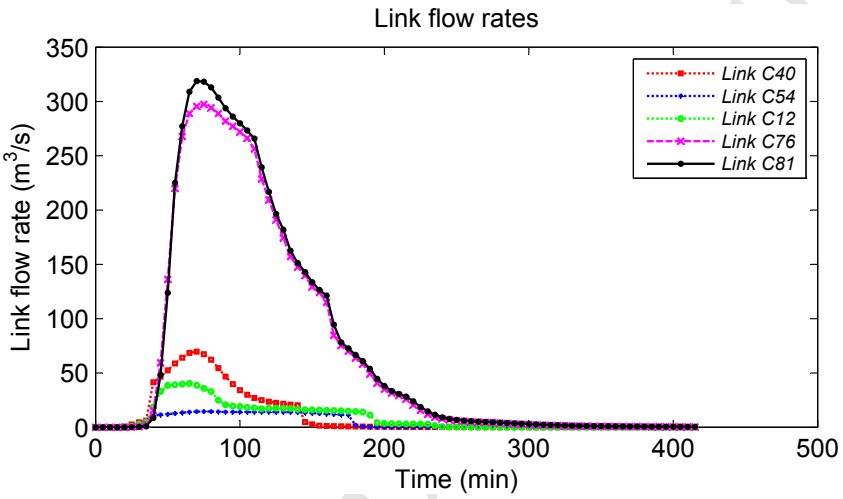


Figure A.3: Simulated flows in the Nakivubo UDS for upstream links C12, C40, C54 and downstream links C76 and C81

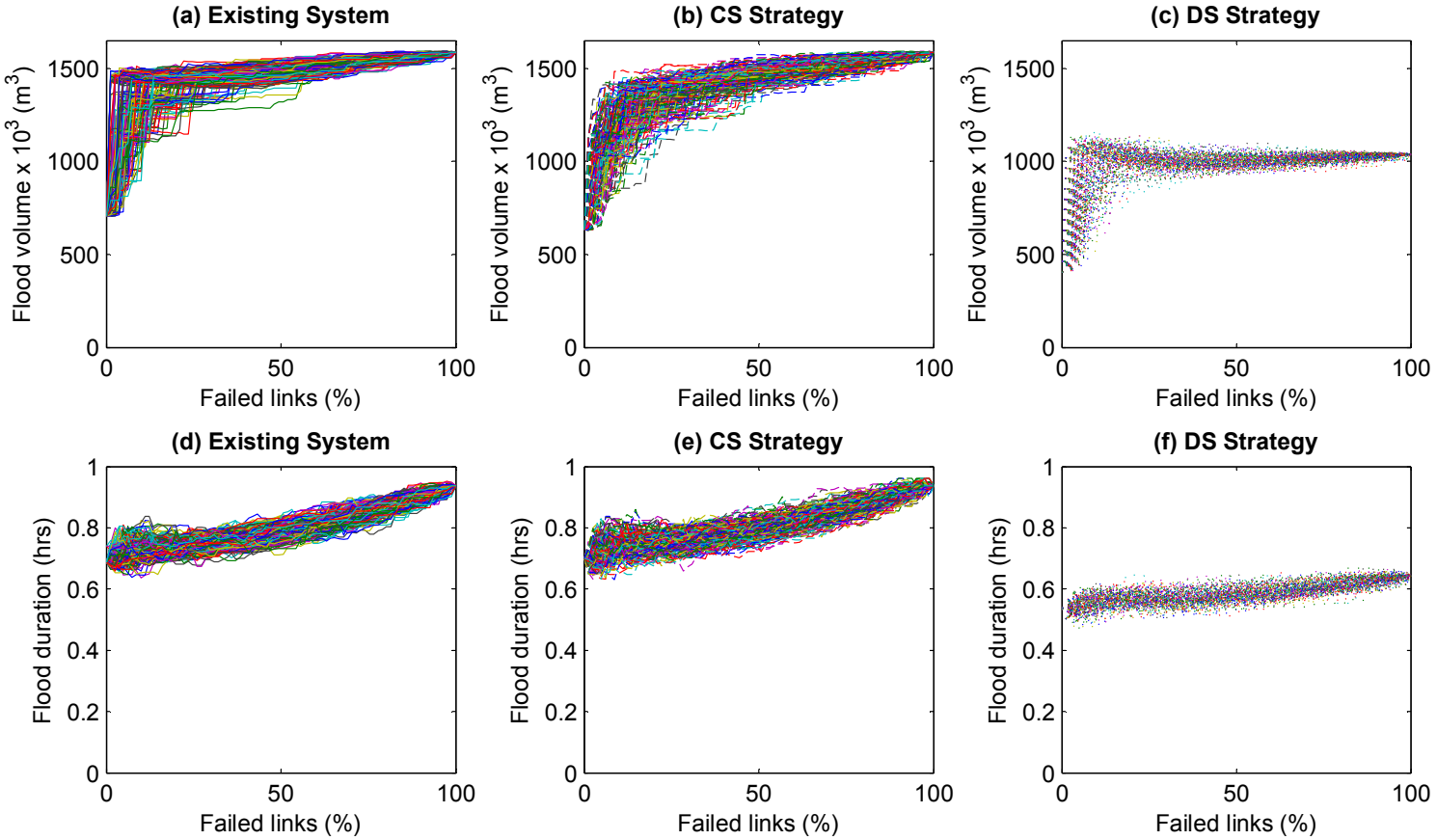


Figure A.4: Effect of random cumulative link failure on total flood volume (a-c) and mean nodal flood duration (d-f). 200 random link failure sequences (16,400 random link failure scenarios) are simulated for the existing UDS ($ns_i$: $i$ = *1,2,3...200*), for the CS Strategy ($cs_i$: $i$ = *1,2,3...200*) and for the DS Strategy ($ds_i$: $i$ = *1,2,3...200*). In total, 49,200 link failure scenarios are simulated.

**Supplementary information**

# A global resilience analysis approach for investigating structural resilience in urban drainage systems

**Seith N. Mugume[a], Diego E. Gomez, Guangtao Fu, Raziyeh Farmani, David Butler**

[a] Centre for Water Systems, College of Engineering, Mathematics and Physical Sciences, University of Exeter, North Park Road, Exeter, EX4 4QF, United Kingdom; Tel: +44 (0)1392 723600, E-mail: snm205@exeter.ac.uk

This supplement contains the following

- Procedure for evaluating the minimum number of random failure sequences $rs_x$ in global resilience analysis
- Figure S1, a figure showing the full sewer failure scenario solution space for an urban drainage system with 81 links, when two system states that is non-failed and completely failed.
- Figure S2, a figure showing the convergence of global resilience analysis results for the case study UDS after 200 random cumulative link failure sequences

## Methods

### 1.1 Evaluating the minimum number of random failure sequences $rs_x$

In order to calculate the maximum possible flooding impacts, all possible link failure scenarios need to theoretically considered (Kellagher, Cesses, Di Mauro, & Gouldby, 2009). Considering two states for each link (i.e. non-failed and complete failure), the total number of link failure scenarios in the entire solution space can be calculated using Equation 1

$$F(N, c_i) = \sum_{i=1}^{i=N} \frac{N!}{(N-i)!i!} \quad (1)$$

Where $F$ is the total number of failure scenarios; $N$ the total number of links and $i$ the link failure level (i.e. number of links failed).

Using an UDS with 81 links as an example and assuming the two link states (non-failed and failed), the total number of failure scenarios would be $2^{81}$ ($2.4 \times 10^{24}$) failure scenarios. In order to minimise the computation resources, it is therefore important to limit the number of scenarios which need to be considered while ensuring accuracy of the modelled flooding impacts (Kellagher et al., 2009). Analysis of the distribution of the number of failure scenarios at each link failure level indicates a normal (Gaussian) distribution (Figure S2). The total number of scenarios involving random failure of a single link (*N-1*) is 81. The total number of scenarios involving random failure of two (*N-2*), three (*N-3*), four (*N-4*) links would be 3,240, 85,320 and 1,663,740 respectively. The highest number of potential failure scenarios occurs at the mid-point i.e. *N-40*.

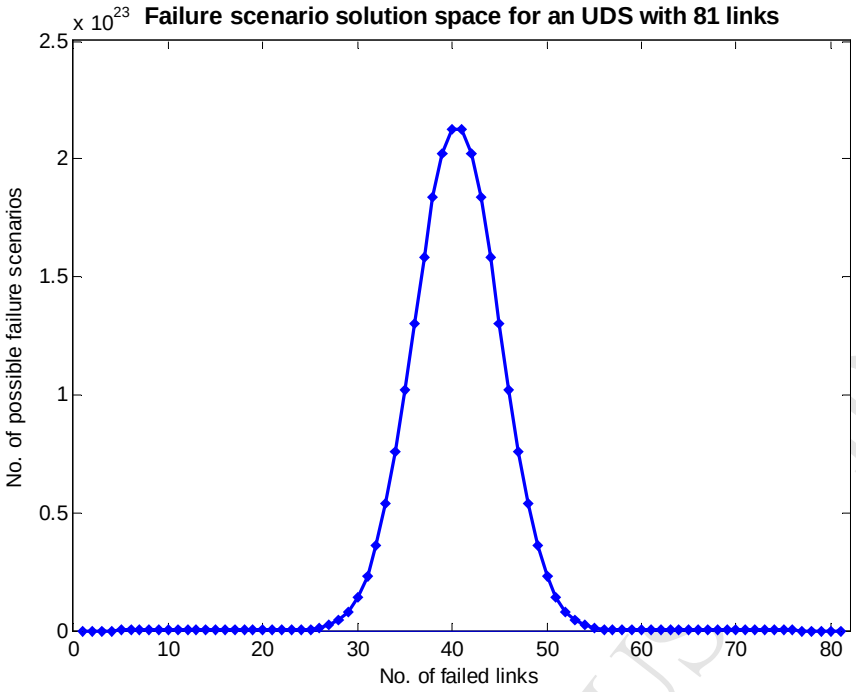


**Figure S1:** Distribution of link failure scenarios at each link failure level

In order to minimise the computational requirements of considering all possible link failure combinations, the minimum number of random failure sequences (hence number of random failure scenarios) that need to analysed in order to achieve convergence of results while covering as many failure states as possible needs to be determined.

Previous studies that employ critical component analysis in networked systems suggest that failure of only a small fraction of components results in the significant impacts on level service delivered by the system (Church & Scaparra, 2007; Johansson & Hassel, 2012; Johansson, 2010). Critical component analysis involves an exhaustive exploration of a system state to estimate negative consequences of failure of a single or set of components (Johansson & Hassel, 2012). In UDSs, critical sewers that is; sewers for which the cost of failure would be significantly higher than upgrading costs make up 20% of the system on average (Butler & Davies, 2011). In this study, critical component analysis of single links (i.e. *i.e. N-1 resilience analysis problem)* is carried out by targeted failure (as opposed to random) of each

individual link in the UDS. The study results suggest that failure of 19.8% of the links in the UDS lead to the highest consequences (Figure S2).

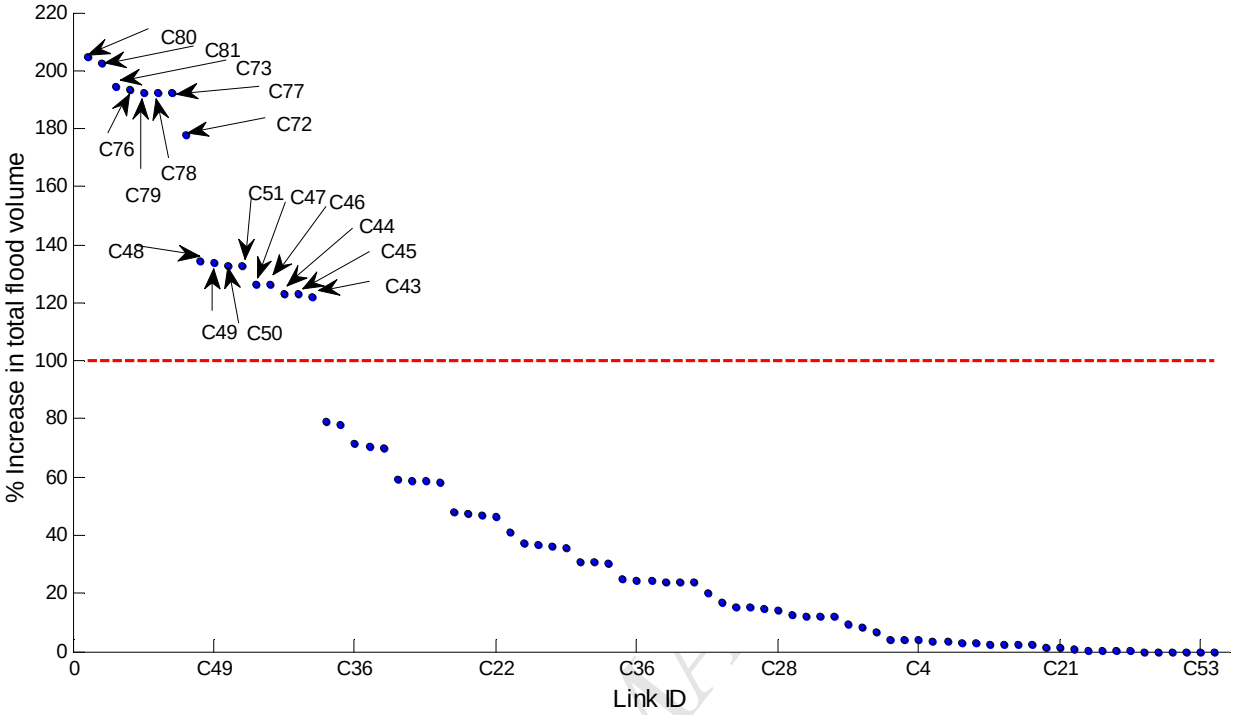


**Figure S2:** Percentage increase in total flood volume resulting from critical component analysis involving single link failure

Based on this, it can be suggested that for a given network, a certain minimum number of random failure sequences, $rs_y$ is necessary to achieve convergence of the GRA results. This ensures that the set of links that are critical are covered in the global resilience analysis (e.g. Johansson & Hassel, 2012). The following steps are carried out to determine $rs_y$ that is required to achieve *convergence* of results:

a) GRA is carried out using 5 random sequences (410 failure scenarios) and the mean values of the total flood volume are determined.

b) The procedure is repeated for 10 (820 failure scenarios), 25 (2050 failure scenarios), 50 (4100 failure scenarios), 100 (8200 failure scenarios), 150 (12,300 failure scenarios) and 200 (16,400 failure scenarios) sequences.

c) The percentage deviation, *PD* the between computed mean values is computed for each step-wise increase in $rs_i$, i.e. for *i:* $i$ = {5,10}; {10, 25}; {25, 50}, {50; 100}, {100;150} and {150;200} (Figure 3)

The results obtained from 5 random sequences indicate the largest variation in the mean values (up to 7.5%) occurs at lower link failure levels (< 10% of the failed links), with convergence occurring at higher links failure levels (Figure S3).

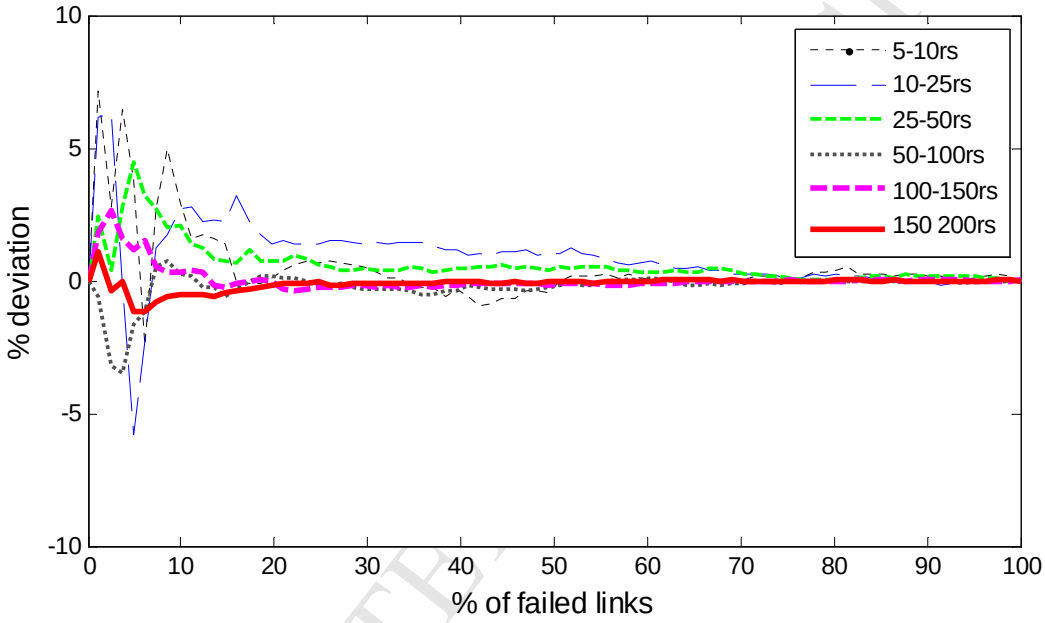


**Figure S3:** Convergence of GRA results after 200 random cumulative failure sequences (rs)

The results also indicate that increasing the number of failure sequences reduces this variation. A convergence is obtained after 50 random failure sequences with a maximum deviation of 4.5%. The maximum deviation is further reduced to 3.5%, 2.6% and 1.1% by considering 100, 150 and 200 random failure sequences respectively. Considering 200 random failure sequences covers all *N-1* (single link) scenarios and covers a statistically significant proportion of *N-2* (two link) scenarios (6.2%) and *N-3* (three link failure) scenarios (0.23%). Consequently, a minimum of 200 random failure sequences is adopted for the GRA. Overall, a total of 49,200 failure scenarios involving 600 random cumulative link

failure sequences are simulated to evaluate the effect on the performance of the existing UDS and the proposed adaptation strategies.

### 1.2 Derivation of the flood resilience index

Figure 2 illustrates the theoretical response of an UDS (in which one or more links have been failed) to a single extreme rainfall loading scenario. Even when one of the links in this UDS has failed, the UDS is able to continue functioning from time to until when the system starts to fail at time $t_{fs}$. A gradual loss of system functionality occurs until when a maximum failure level is reached at time $t_{mf}$. After occurrence of the extreme rainfall, hydraulic capacity in the UDS is gradually restored to original or lower but acceptable levels.

The concept of *severity* (Hwang, Lansey, & Quintanar, 2015) which is a defined as the level of consequences (e.g. injury, property or system damage) that could result from occurrence given failure mode or threat is used as a measure of the resulting *loss of system functionality* when the UDS is subjected to a given exceptional loading scenario that leads to failure. It can be estimated as the (shaded) area between the original system performance level ($P_o$) and the actual system performance curve, $P_i(t)$, which represents the *magnitude* of the loss of functionality for the system being tested (Figure 4). The peak severity, $Sev_p$ is a time independent function of system performance and represents the maximum possible *magnitude of loss of functionality* when the UDS is subjected to a given threat. The system wide theoretical peak severity, $Sev_p$ is given by Equation 3.

$$Sev_p = \left(\frac{P_o - P_f}{Po}\right) \tag{3}$$

Where $P_o$ is the original system performance level before system failure (i.e. no flooding) and $P_f$ is the lowest performance level of the system after failure i.e. the maximum possible total flood volume.

The system failure impact duration, $t_f$ provides an estimate of the recovery time. The recovery time is defined as the time period between the onset of system failure, $t_{fs}$ (i.e. when system functionality drops below the original levels) and the return time to the original or lower but acceptable system performance levels (Lansey, 2012; Wang & Blackmore, 2009). In this study, it is estimated using the mean flood duration that is the time interval between the onset and subsidence of nodal flooding (Equation 4).

$$t_f = f[t_r - t_{fs}] \quad (4)$$

Where $t_{fs}$ is time of start of flooding and $t_r$ is the return time to original system functionality (end of surface flooding).

In practice, however, the recovery time is dependent on other factors that are generally external to the physical design and layout of a system that is resourcefulness and rapidity. Resourcefulness is defined as the ability to respond to a failure event (Lansey, 2012). It is a measure of the capacity to identify failures, establish priorities and mobilize resource in the event disruptions resulting from system failure (Wang & Blackmore, 2009). Rapidity on the other hand is defined as the speed at which resources are deployed to restore acceptable functionality levels (Lansey, 2012). In this study, focus is placed on quantifying the influence of inbuilt system properties/attributes on UDS resilience to flooding. Based on this premise, resourcefulness and rapidity have been excluded from the estimation of recovery time.

To estimate the resulting loss of system functionality as function of failure magnitude and duration, *volumetric severity*, $Sev_i$, which is function of the peak severity and the failure duration is computed using Equation 3.

$$Sev_i = f\left[Sev_p,\ t_f\right] = \frac{1}{P_o}\int_{t_o}^{t_n}(P_o - P_i(t))dt \quad (3)$$

Where $Sev_i$ is the severity, $t_f$ the time of failure, $t_o$ the start time of the simulation and $t_n$ the total elapsed time.

To simplify the integration Equation 3 above, a rectangular shape of the system failure and recovery is assumed (Equation 4)

$$Sev_i = \frac{V_{TF}}{V_{TI}} \times \frac{t_r - t_{fs}}{t_n - t_o} = \frac{V_{TF}}{V_{TI}} \times \frac{t_f}{t_n} \quad (4)$$

Finally, the resilience index, $Res_o$, which is a measure of system residual functionality, is estimated as one minus the computed volumetric severity and is computed at each link failure level (Equation 5).

$$Res_o = 1 - Sev_i = 1 - \frac{V_{TF}}{V_{TI}} \times \frac{t_f}{t_n} \quad (5)$$

Where $V_{TF}$ is the total flood volume, $V_{TI}$ the total inflow into the system, $t_f$ the mean duration of nodal flooding and $t_n$ the total elapsed (simulation) time.